Journal of Power Sources 183 (2008) 766–770

Contents lists available at ScienceDirect

Journal of Power Sources

journal homepage: www.elsevier.com/locate/jpowsour

Short communication

Structural and thermal properties of $LiNi_{0.6-x}Mg_xCo_{0.25}Mn_{0.15}O_2$ cathode materials

Pei-Yun Liao [a], Jenq-Gong Duh [a,*], Hwo-Shuenn Sheu [b]

[a] Department of Materials Science and Engineering, National Tsing Hua University, Hsinchu, Taiwan
[b] National Synchrotron Radiation Research Center, Hsinchu Science-Based Industrial Park, Hsinchu, Taiwan

ARTICLE INFO

Article history:
Received 28 February 2008
Received in revised form 9 May 2008
Accepted 19 May 2008
Available online 28 May 2008

Keywords:
Li-ion battery
Cathode
Layered structure
In situ XRD

ABSTRACT

For improving the electrochemical performance and thermal stability, magnesium was chosen as the doping element in $Li(NiCoMn)O_2$ cathode materials. $LiNi_{0.6-x}Mg_xCo_{0.25}Mn_{0.15}O_2$ ($x = 0$ and 0.03) were successfully synthesized via the mixing hydroxide method. These materials exhibited α-$NaFeO_2$ structure as indicated by the XRD patterns. The intensity ratio of (0 0 3) to (1 0 4) showed that the Mg substitution could reduce the cation mixing. The pristine material exhibited the initial discharge of capacity 199 mAh g^{-1} and remained retention of 79% after 20 cycles in the voltage range of 3–4.5 V. When magnesium ions were substituted, the initial capacity was reduced due to the less active ions. However, the capacity retention was increased to 95%. Not only cycleability, but also the thermal stability was improved by Mg substitution at every delithiated state of electrodes with electrolytes. The in situ synchrotron X-ray diffraction patterns showed that the boundary of phase transition for H1 to H2 was much clearer in Mg-doped sample, indicating that the $LiNi_{0.57}Mg_{0.03}Co_{0.25}Mn_{0.15}O_2$ material exhibited higher structural integrity. The improvements of both electrochemical retention and thermal stability were possibly attributed to the reduced cation mixing and complete structural changes.

1. Introduction

Rechargeable Li-ion batteries with high energy density have become the most promising power sources for a variety of portable electronic devices since the first commercialization of the battery in 1991 by Sony [1]. Recently, many materials which are cost-effective, safe and environment friendly compared with the widely used commercial $LiCoO_2$ cathode have been investigated [2–6]. One of the most attractive materials is $LiNi_{1-x}Co_xMn_yO_2$, which is a solid solution of $LiNiO_2$, $LiCoO_2$, and $LiMnO_2$ [5–9]. The material possesses a α-$NaFeO_2$ structure, consisting of close-packed oxygen ions in the ABCABC arrangement (O3 stacking type) with Li and transition metal ions in the alternate layers. Ohzuku reported that the $LiNi_{1/3}Co_{1/3}Mn_{1/3}O_2$ had a capacity of 200 mAh g^{-1} in the voltage window of 2.5–4.6 V [6–7]. Recently, $LiNi_{0.75-x}Co_{0.25}Mn_xO_2$ ($x = 0.1$–0.25) materials synthesized by the mixing hydroxide method also showed satisfied capacities and the rate capability [9]. $LiNi_{0.6}Co_{0.25}Mn_{0.15}O_2$ exhibited the discharge capacity of 167 and 150 mAh g^{-1} at $C/10$ and 1C rate during 3–4.3 V, respectively [9]. However, the material still had some short-comings, such as the large initial irreversible capacity, low electronic conductivity and instability of Ni ions.

In literatures, many attempts have been made to improve the performance of cathode materials [10–13]. One approach is the cationic substitution for transition metal ions. Lee et al. reported that Al doping could increase the capacity retention for long-term cycling at elevated temperature [12]. In addition, cationic substitution for nickel to form substituted $LiNi_{1-x}M_xO_2$ (M = Fe, Mg, Al and Ti) could stabilize the Ni-based oxide and appeared to be a good method to modify the structural and electrochemical performance [10,14–17]. In the present work, Mg was chosen as the doping element in $LiNi_{0.6-x}Mg_xCo_{0.25}Mn_{0.15}O_2$ ($x = 0$ and 0.03) and detailed studies such as the cation mixing and structural change during charge were conducted to verify the stabilizing effect of magnesium. Besides, the safety issue has currently become a serious concern to evaluate the electrode materials for Li-ion batteries. Thermal behavior also was thus discussed using differential scanning calorimetry (DSC) in this work.

2. Experimental

$[Ni_{0.6-x}Mg_xCo_{0.25}Mn_{0.15}O_2](OH)_2$ ($x = 0$ and 0.03) powders were synthesized by the previously reported co-precipitation method [9]. The aqueous solution of $NiSO_4{\cdot}6H_2O$, $CoSO_4{\cdot}7H_2O$, $MnSO_4$

* Corresponding author. Tel.: +886 3 5712686; fax: +886 3 5712686.
E-mail address: jgd@mx.nthu.edu.tw (J.-G. Duh).

0378-7753/$ – see front matter © 2008 Elsevier B.V. All rights reserved.
doi:10.1016/j.jpowsour.2008.05.058

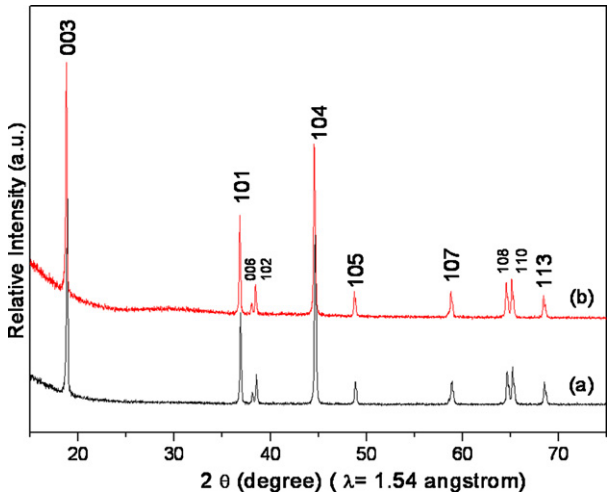

Fig. 1. XRD patterns for (a) $LiNi_{0.6}Co_{0.25}Mn_{0.15}O_2$ and (b) $LiNi_{0.57}Mg_{0.03}Co_{0.25}Mn_{0.15}O_2$ powders.

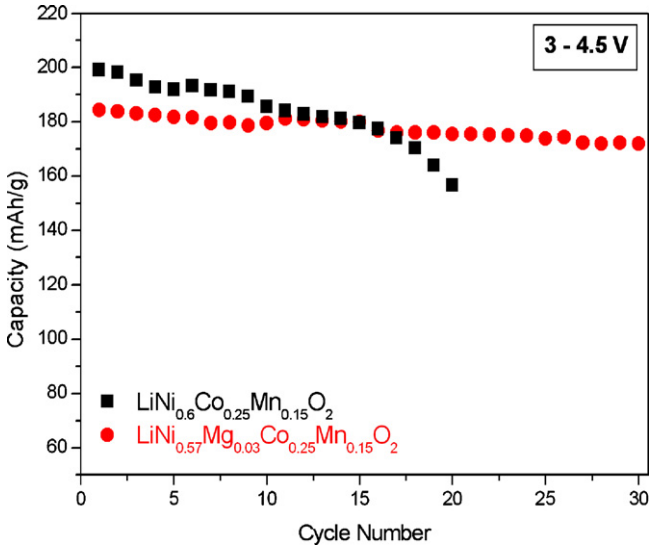

Fig. 3. The discharge capacity as a function of cycle number for the $LiNi_{0.6}Co_{0.25}Mn_{0.15}O_2$ and $LiNi_{0.57}Mg_{0.03}Co_{0.25}Mn_{0.15}O_2$ cells between 3 and 4.5 V.

and $MgSO_4$ was slowly pumped into the reactor, and meanwhile the aqueous solutions of NH_4OH and NaOH were also fed into the solution at a constant rate to adjust the pH value at 12. The filtrated precipitate was washed several times to ensure that the residual ions (Na^+, SO_4^{2-} or others) were almost removed. The $[Ni_{0.6-x}Mg_xCo_{0.25}Mn_{0.15}O_2](OH)_2$ ($x = 0$ and 0.03) product was dried, then mixed with Li_2CO_3 in ethanol using a mortar and pestle, and heated to 900 °C for 15 h in the flowing O_2 to obtain $Li[Ni_{0.6-x}Mg_xCo_{0.25}Mn_{0.15}O_2]O_2$ ($x = 0$ and 0.03) powders.

The phase of prepared powders was analyzed with an X-ray diffractometer (Shimadzu X-ray diffractometer XRD-6000, Japan) operated at 40 kV and 30 mA from 15° to 75° with a wavelength of Cu Kα (λ = 1.5406 Å). On the basis of the XRD results, the lattice parameters were calculated by the least-square method with ten diffraction lines.

The electrodes were fabricated with a mixture of 89 wt.% cathode powder, 2 wt.% super P, 4 wt.% KS6, and 5 wt.% polyvinylidene difluoride (PVDF) binder in *N*-methyl-2-pyrrolidone (NMP) to obtain a slurry. 1 M $LiPF_6$ in a 1:2 (volume ratio) mixture of EC/DMC was used as the electrolyte. Type 2016 coin-cells (20 mm in diameter and 1.6 mm thick) were assembled with the Li foil as an anode in an argon glove box where both moisture and oxygen content were <1 ppm. The mass of the electrodes was 23–25 mg. The cells were cycled in the voltage range of 3–4.5 V with a constant current of 0.33 mA (CCCV mode).

The cell designation of in situ XRD experiments was similar to the regular one for the electrochemical test. To have in situ X-ray pass through the cathode electrode, holes with 4φ were drilled in the upper cover, bottom cover and Ni spacer of the 2016 coin cell and followed by sealing with a Kapton film. In situ X-ray studies were carried out in the transmission mode at 16 keV (λ = 0.775 Å) in the National Synchrotron Radiation Research Center (NSRRC), Taiwan. The exposure time was 6 min and XRD spectra were recorded on the Mar 345-image plate detector. All in situ X-ray diffraction patterns were calibrated using standard sample (Ag + Si) before further analysis.

The charging method for DSC measurement was referred to that reported by Dahn and co-workers [18]. The cells were charged to

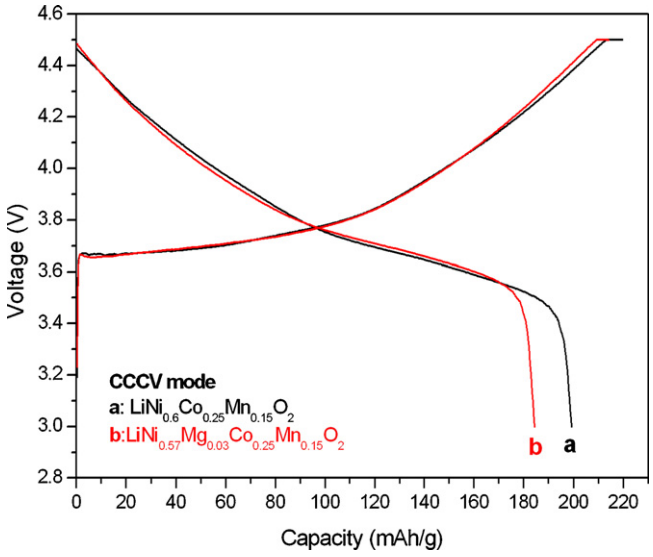

Fig. 2. The first charge and discharge profiles of (a) $LiNi_{0.6}Co_{0.25}Mn_{0.15}O_2$ and (b) $LiNi_{0.57}Mg_{0.03}Co_{0.25}Mn_{0.15}O_2$ between 3 and 4.5 V at *C*/10 rate.

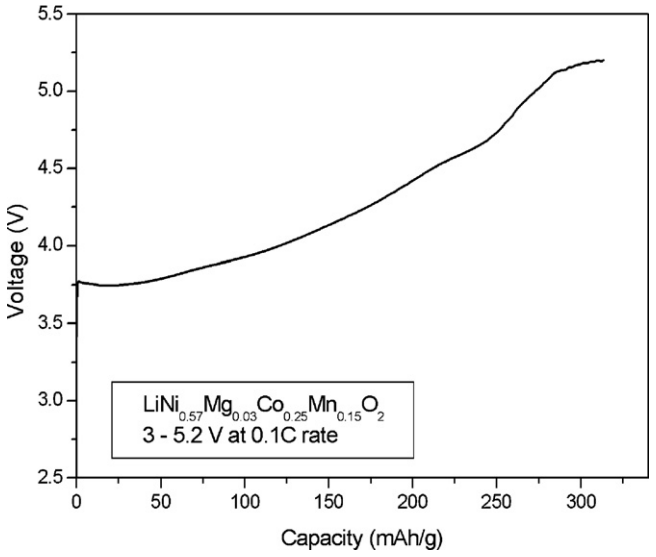

Fig. 4. The first charge curve for the in situ $LiNi_{0.57}Mg_{0.03}Co_{0.25}Mn_{0.15}O_2$ cell from 3 to 5.2 V at *C*/10 rate.

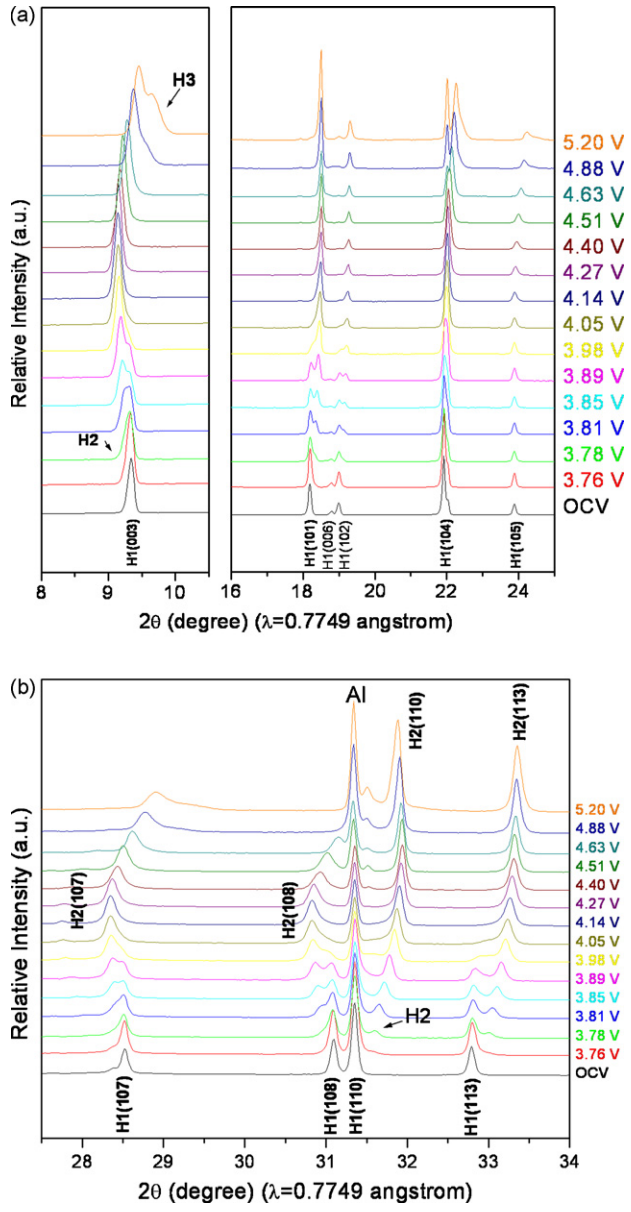

Fig. 5. In situ XRD patterns of $LiNi_{0.57}Mg_{0.03}Co_{0.25}Mn_{0.15}O_2$ cell charged to 5.2 V in the 2θ region of (a) (0 0 3) to (1 0 5), and (b) (1 0 7) to (1 1 3).

desired voltages (4.1–4.7 V) with a specific current of 0.1*C*. When the cell reached this voltage, the current was stopped for 30 min (rest mode). Then the cell was re-charged with a current of 80% of the previous one. This cycling method would be repeated for 12 times to ensure the stable desired voltage. After the charging cycle, the cell was disassembled in the glove box and the material was sealed in the Al pan. Measurements were carried out with a differential scanning calorimeter (Perkin Elmer, DSC7, USA) at a scan rate of 2 °C min^{-1} in Ar atmosphere.

3. Results and discussion

The X-ray diffraction patterns of the pristine $LiNi_{0.6}Co_{0.25}Mn_{0.15}O_2$ and Mg-doped $LiNi_{0.57}Mg_{0.03}Co_{0.25}Mn_{0.15}O_2$ are shown in Fig. 1. The patterns were the characteristic of a hexagonal α-$NaFeO_2$ structure (space group: *R*-3*m*, No. 166) in which oxygen ions were in a close-packed FCC array, while Li and transition metal ions occupied the 3a and 3b octahedral sites, respectively, on the alternate (1 1 1) plane. The obvious splits of (0 0 6 and 1 0 2) and (1 0 8 and 1 1 0) couples suggested an ordering layered-structure for both of them. The intensity ratio of the (0 0 3) to (1 0 4) lines was sensitive to the degree of cation mixing [19], in which the larger $I_{(003)}/I_{(104)}$ ratio indicated the less cation mixing between Li and Ni ions. As Mg was doped in $LiNi_{0.57}Mg_{0.03}Co_{0.25}Mn_{0.15}O_2$, the ratio increased from 1.32 to 1.46, implying that the cation mixing was reduced. It meant that Mg ions could prevent the occupancy of Li^+ layers by Ni ions and did not cause the local structural collapse. The calculated lattice constants of $LiNi_{0.6}Co_{0.25}Mn_{0.15}O_2$ were $a = 2.863$ Å and $c = 14.189$ Å, which increased to $a = 2.864$ Å and $c = 14.203$ Å for $LiNi_{0.57}Mg_{0.03}Co_{0.25}Mn_{0.15}O_2$. Therefore, the unit cell volume also increased from 100.721 to 100.893 $Å^3$. This might be attributed to the substitution of Ni^{2+} ($r^{2+}_{Ni} = 0.69$ Å) with the larger ionic radius Mg^{2+} ions ($r^{2+}_{Mg} = 0.72$ Å).

Fig. 2 shows the initial charge–discharge curves of $LiNi_{0.6}Co_{0.25}Mn_{0.15}O_2$ and $LiNi_{0.57}Mg_{0.03}Co_{0.25}Mn_{0.15}O_2$ samples. The cells were charged at constant current of *C*/10 rate to the desired voltages of 4.5 V, followed by constant voltage for 2 h (CCCV mode), and then discharged to 3 V at constant *C*/10 rate. As shown in Fig. 2, the initial discharge capacity of Mg-doping $LiNi_{0.57}Mg_{0.03}Co_{0.25}Mn_{0.15}O_2$ decreased from 199 to 184 mAh g^{-1} as compared with un-doped one. To the best of our knowledge, the main redox reaction in nickel-based cathode materials during delithiation was achieved by Ni ions. In our previous study of valence changes by XAS measurements, it was deduced that the charge compensation was mainly by two-step oxidation of Ni ions: Ni^{2+} to Ni^{3+} during 3–3.9 V and then Ni^{3+} to Ni^{4+} in the higher voltage of 3.9–4.5 V [20]. Therefore, electrochemically inactive Mg substitution for active Ni ions would result in the decrease of capacity. The cyclic performance tested in the voltage range of 3–4.5 V is presented in Fig. 3. Although the initial capacity of $LiNi_{0.6}Co_{0.25}Mn_{0.15}O_2$ was larger than that of $LiNi_{0.57}Mg_{0.03}Co_{0.25}Mn_{0.15}O_2$, the capacity after 20 cycles was only 157 mAh g^{-1}, which was corresponding to 79% retention. However, the $LiNi_{0.57}Mg_{0.03}Co_{0.25}Mn_{0.15}O_2$ sample exhibited 95% retention, which was much higher than that of pristine $LiNi_{0.6}Co_{0.25}Mn_{0.15}O_2$. This indicated that the Mg substitution possessed a positive effect on the capacity retention and would improve the cycleability in this type of materials.

In literature, it was reported that the enhanced cycling stability of Mg substitution samples was attributed to the Mg ions incorporation into LiO_2 layers due to the similar ionic size of Li^+ and Mg^{2+}. The presence of Mg^{2+} in lithium sites would prevent local collapse, help lithium diffusion and therefore resulted in an increase of the capacity retention [10,17,21]. Here, another interesting point on the basis of structural changes during cycling is referred to explain the increase of cycleability. The structural stability of Mg-doped system was investigated by the in situ synchrotron XRD study. Fig. 4 shows the first charging curve for the in situ $LiNi_{0.57}Mg_{0.03}Co_{0.25}Mn_{0.15}O_2$ cell charged to 5.2 V at the current of *C*/10 rate (about 0.29 mA). Fig. 5(a) and (b) shows the evolution of XRD patterns with the corresponding voltages during cycling in the 2θ ranging from (0 0 3) to (1 0 5) and (1 0 7) to (1 1 0), respectively. The XRD pattern at open-circuit voltage (OCV, around 3.4 V) was identical with that of pristine powder in Fig. 1(b). By tracking the variation of (0 0 3) peak, three hexagonal phases (H1, H2 and H3) could be identified during charge and their corresponding Bragg peaks were indexed, as indicated in Fig. 5. The process of phase change in this work is similar with those in nickel-based layer-structured cathode materials, such as $LiNiO_2$ [22], $LiMn_{0.5}Ni_{0.5}O_2$ [23] and $Li_xNi_{0.89}Al_{0.16}O_2$ [24]. The phase transition from H1 to H2 could be clearly observed to start at 3.78 V. The H2 phase exhibited the same hexagonal structure as the H1 phase at OCV, however, the larger *c* lattice constant

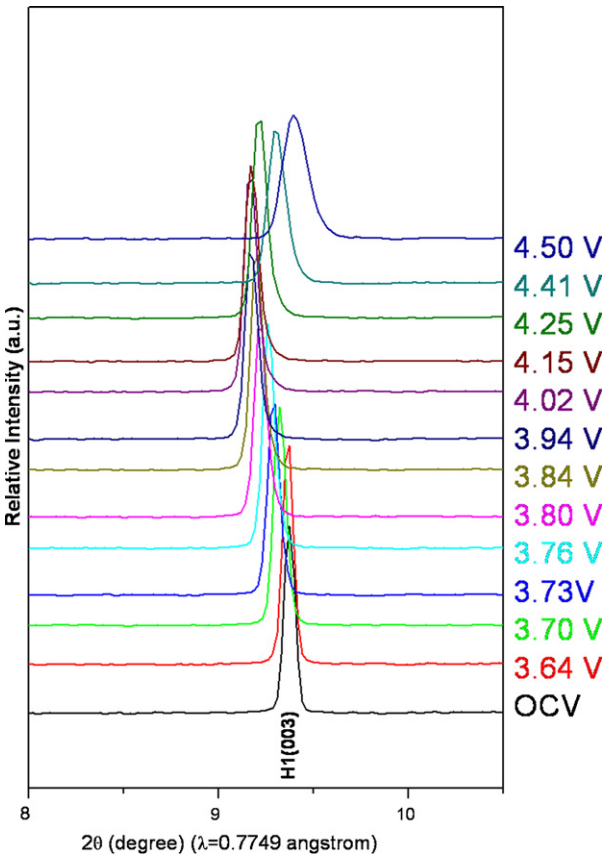

Fig. 6. The evolution for (0 0 3) peak in the in situ XRD patterns for $LiNi_{0.6}Co_{0.25}Mn_{0.15}O_2$ cell charged to 4.5 V.

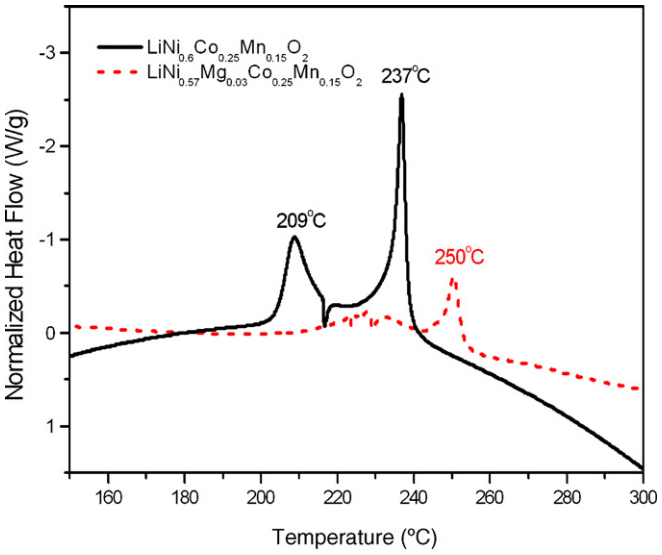

Fig. 7. DSC tests of $LiNi_{0.6}Co_{0.25}Mn_{0.15}O_2$ and $LiNi_{0.57}Mg_{0.03}Co_{0.25}Mn_{0.15}O_2$ electrodes after charging to 4.5 V. The scan rate was 2 °C min^{-1}.

and smaller a lattice constant were revealed due to the lower angle of $(0\,0\,3)_{H2}$ and higher angle of $(1\,1\,0)_{H2}$ as compared with $(0\,0\,3)_{H1}$ and $(1\,1\,0)_{H1}$, respectively. During the voltage ranging from 3.78 to 4.14 V, the position of $(0\,0\,3)_{H2}$ continuously shifted to lower angle attributing to the expansion of *c*-axis for H2 phase, while the position of $(0\,0\,3)_{H1}$ remained the same. When charged to higher voltage above 4.14 V, the $(0\,0\,3)_{H1}$ peak was hardly observed, meaning the disappearance of the original H1 phase. At the same time, the $(0\,0\,3)_{H2}$ peak moved towards the higher angle substantially and formed a new $(0\,0\,3)_{H3}$ shoulder at around 5.2 V. It is interesting to note that the formation of H3 phase was an indicator for thermal stability [22,25–26], where the H2 to H3 phase transition occurred at 4.3 V in $LiNiO_2$ [22]. The suppression of H3 phase for $LiNi_{0.57}Mg_{0.03}Co_{0.25}Mn_{0.15}O_2$ in this study was expected to achieve a better thermal stability.

Fig. 6 focuses on the change of (0 0 3) reflection for un-doped $LiNi_{0.6}Co_{0.25}Mn_{0.15}O_2$ charged to 4.5 V at *C*/10 current rate. The complete in situ XRD patterns were already reported elsewhere [27] and only the evolution of (0 0 3) reflection is shown here for comparison. The (0 0 3) peak of original H1 phase shifted to lower angle during OCV to 4.15 V. Then towards the end of charge there was a major shift to higher angle (4.15–4.5 V) with a simultaneous peak broadening near 4.4 V. A comparison of the evolution for (0 0 3) between $LiNi_{0.6}Co_{0.25}Mn_{0.15}O_2$ and $LiNi_{0.57}Mg_{0.03}Co_{0.25}Mn_{0.15}O_2$ showed that the boundary of phase transition from H1 to H2 was smeared and hardly identified in bare $LiNi_{0.6}Co_{0.25}Mn_{0.15}O_2$ as shown in Fig. 6. Base on literatures [16,22,28] and our previous in situ XRD studies for a series of $LiNi_{0.75-x}Co_{0.25}Mn_xO_2$ ($x = 0.1$–0.25) materials [20,27], it was revealed that the smeared phase transition was attributed to the lattice defects. Therefore, the evident and complete phase transition in $LiNi_{0.57}Mg_{0.03}Co_{0.25}Mn_{0.15}O_2$ confirmed the stabilizing effect of Mg. Doping a small amount of Mg could increase the structural integrity. This might be the reason that the capacity retention was raised by Mg-doping as previously shown in Fig. 3.

Differential scanning calorimetry (DSC) measurements of $LiNi_{0.6}Co_{0.25}Mn_{0.15}O_2$ and $LiNi_{0.57}Mg_{0.03}Co_{0.25}Mn_{0.15}O_2$ charged to 4.5 V is shown in Fig. 7. The $LiNi_{0.6}Co_{0.25}Mn_{0.15}O_2$ material exhibited two exothermic peaks: a weak centered at 209 °C with an onset temperature of 200 °C followed by a large peak at 237 °C. It produced 772 J g^{-1} of heat roughly. However, with the Mg-doped $LiNi_{0.57}Mg_{0.03}Co_{0.25}Mn_{0.15}O_2$, a broad peak with the onset temperature of 210 °C and only one major peak at 250 °C were observed. In addition, the exothermic reaction of $LiNi_{0.57}Mg_{0.03}Co_{0.25}Mn_{0.15}O_2$ was milder due to the less heat released (450 J g^{-1}). Fig. 8 shows the respective exothermic temperature plotted versus the state of delithiation *x* in electrodes. There was an approximately linear cor-

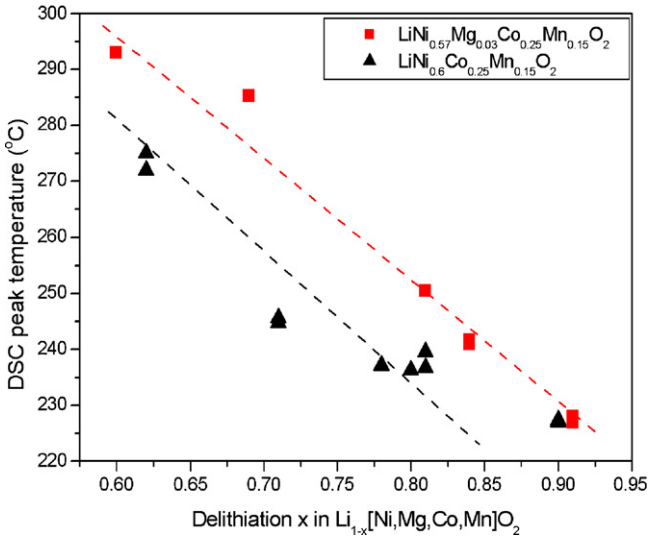

Fig. 8. The exothermic temperature as a function of delithiation *x* in $Li_{1-x}Ni_{0.6}Co_{0.25}Mn_{0.15}O_2$ and $Li_{1-x}Ni_{0.57}Mg_{0.03}Co_{0.25}Mn_{0.15}O_2$ electrodes.

relation between temperature and state of delithiation, and the exothermic temperature shifted to the lower side as Li content decreased. By doping Mg in $LiNi_{0.6}Co_{0.25}Mn_{0.15}O_2$, the exothermic reactions were remarkably suppressed and the decomposition temperature at any lithium content could be effectively raised. The DSC results clearly demonstrated that thermal stability of the charged cathode material with electrolytes was significantly improved by Mg substitution.

4. Conclusion

$LiNi_{0.6-x}Mg_xCo_{0.25}Mn_{0.15}O_2$ ($x = 0$ and 0.03) cathode materials were successfully synthesized by the mixing hydroxide method. By the intensity ratio of (0 0 3) to (1 0 4) in the XRD patterns, it was found that the Mg substitution could reduce the cation mixing. The pristine material exhibited the initial discharge of capacity 199 mAh g^{-1} and remained retention of 79% after 20 cycles in the voltage range of 3–4.5 V. The Mg substituted $LiNi_{0.57}Mg_{0.03}Co_{0.25}Mn_{0.15}O_2$ showed the capacity retention higher than 95% due to the less cation mixing and higher structural integrity for clear boundary of phase transition as indicated by the in situ synchrotron XRD studies. The Mg substituted $LiNi_{0.57}Mg_{0.03}Co_{0.25}Mn_{0.15}O_2$ also showed an increase in thermal stability of charged electrodes with electrolytes.

Acknowledgments

The authors are grateful to the Coremax Taiwan Corporation and the National Science Council, Taiwan (No. NSC 96-2221-E-007-093) for the partial financial support. We also thank J.J. Lee and W.T. Chuang for their technical assistance and the National Synchrotron Radiation Research Center (NRSSC) for use of their synchrotron X-ray diffraction facilities.

References

[1] M. Inaba, Z. Ogumi, Up-to-date development of lithium-ion batteries in Japan, IEEE Electr. Insul. Mag. 17 (2001) 6.
[2] C. Saadoune, J. Delmas, Solid State Chem. 136 (1998) 8.
[3] C.C. Chang, P.N. Kumta, J. Power Sources 75 (1998) 44.
[4] A.K. Padhi, K.S. Nanjundaswamy, J.B. Goodenough, J. Electrochem. Soc. 144 (1997) 1188.
[5] D.D. MacNeil, X. Lu, J.R. Dahn, J. Electrochem. Soc. 149 (2002) A1332.
[6] T. Ohzuku, Y. Makimura, Chem. Lett. (2001) 642.
[7] N. Yabuuchi, T. Ohzuku, J. Power Sources 119–121 (2003) 171.
[8] S.H. Park, C.S. Yoon, S.G. Kang, H.S. Kim, S.I. Moon, Y.K. Sun, Electrochim. Acta 49 (2004) 557.
[9] P.Y. Liao, J.G. Duh, S.R. Sheen, J. Electrochem. Soc. 152 (9) (2005) A1695.
[10] C. Pouillerie, L. Croguennec, Ph. Biendan, P. Willmann, C. Delmas, J. Eelectrochem. Soc. 147 (6) (2000) 2061.
[11] S.B. Jang, S.H. Kang, K. Amine, Y.C. Bar, Y.K. Sun, Electrochim. Acta 50 (2005) 4168.
[12] K.S. Lee, S.T. Myung, H.J. Bang, S. Chung, Y.K. Sun, Electrochim. Acta 52 (2007) 5201.
[13] H.W. Chan, J.G. Duh, J.F. Lee, Electrochem. Commun. 8 (2006) 1731.
[14] R. Kanno, T. Shirane, Y. Inaba, Y. Kawamoto, J. Power Sources 68 (1997) 145.
[15] T. Ohzuku, A. Ueda, M. Kouguchi, J. Electrochem. Soc. 142 (1995) 4033.
[16] W.S. Yoon, K.Y. Chung, M. McBreen, X.Q. Yang, Electrochem. Commun. 8 (2006) 1257.
[17] C.C. Chang, J.Y. Kim, P.N. Kumta, J. Electrochem. Soc. 147 (5) (2000) 1722.
[18] D.D. MacNeil, Z. Lu, Z. Chen, J.R. Dahn, J. Power Sources 108 (2002) 8.
[19] T. Ohzuku, A. Ueda, M. Nagayama, J. Electrochem. Soc. 140 (1993) 1862.
[20] P.Y. Liao, J.G. Duh, J.F. Lee, H.S. Sheu, Electrochim. Acta 53 (2007) 1850.
[21] M. Mladenov, R. Stoyanova, E. Zhecheva, S. Vassilev, Electrochem. Commun. 3 (2001) 410.
[22] X.Q. Yang, X. Sun, J. McBreen, Electrochem. Commun. 1 (1999) 227.
[23] X.Q. Yang, J. McBreen, W.S. Yoon, C.P. Grey, Electrochem. Commun. 4 (2002) 649.
[24] M. Guilmard, A. Rougier, M. Grüne, L. Croguennec, C. Delmas, J. Power Sources 115 (2003) 305.
[25] W. Li, J.N. Reimers, J.R. Dahn, Solid State Ionics 67 (1993) 123.
[26] L. Wang, T. Maxisch, G. Ceder, Chem. Mater. 19 (3) (2007) 543.
[27] P.Y. Liao, J.G. Duh, H.S. Sheu, Electrochem. Solid-State Lett. 10 (4) (2007) A88.
[28] N. Yabuuchi, Y. Koyama, N. Nakayama, T. Ohzuku, J. Electrochem. Soc. 152 (2005) A1434.